JOURNAL OF GUIDANCE, CONTROL, AND DYNAMICS
Vol. 22, No. 5, September–October 1999

Floquet Approximation for a Nearly Axisymmetric Rigid Body with Constant Transverse Torque

R. Anne Gick,* Marc H. Williams,† and James M. Longuski‡
Purdue University, West Lafayette, Indiana 47907-1282

We use Floquet theory to solve the problem of large angular excursions of the spin axis of a rigid body. A semi-analytic solution is presented for the attitude motion of a spinning nearly axisymmetric spacecraft subject to constant transverse torques. Based on the assumption that the spin rate remains nearly constant, we employ a Cayley–Klein representation of the kinematic equations to cast them as a linear set of differential equations with periodic coefficients. The attitude solutions are computed using Fourier series expansions. For cases where the applied torque is small enough, we present a simple approximate solution. In addition, a lower bound is given for the truncation level of the Fourier series. For the axisymmetric case (where the assumption of constant spin rate is exact), highly accurate solutions can be obtained with relatively few Fourier terms for typical spacecraft maneuvers with purely transverse torque. However, when the solution is applied to the nearly axisymmetric case, the errors are driven by the variation in the spin rate.

Introduction

SINCE Grammel defined the problem of the self-excited rigid body, numerous investigators[1–9] have contributed approximate analytic solutions for its motion. The body is free to rotate about a point fixed in the body and inertial space under the action of a torque vector arising from internal reactions that do not appreciably alter the mass or mass distribution. The forced motion of a spacecraft due to thruster torques is a particularly relevant, modern example of the self-excited rigid body.

In the literature a number of simplifying assumptions are used to put the nonlinear differential equations involved into tractable form for analytic integration. In dealing with Euler's equations of motion, most authors assume the body is axisymmetric (or nearly axisymmetric) and that the body-fixed torque components (which may act on up to three axes) are constants. To solve the associated kinematic differential equations, the usual approach is to use Eulerian angles and then to make small angle approximations (for example, on two of the angles) to obtain approximate, closed-form analytic solutions. Recently, interest has been stimulated in other attitude representations (see the excellent survey paper by Shuster[10]). A new parameterization developed by Tsiotras and Longuski[11] has been employed to find an approximate solution[8] for large-angle motion of an axisymmetric or nearly axisymmetric rigid body due to constant torque about three body axes. No exact solution is known (even for the axisymmetric case) of constant torque on three axes.

In this paper we show that the axisymmetric case of constant transverse torque, i.e., no axial torque, is amenable to Floquet theory[12,13] when Cayley–Klein parameters[10,14] are used for attitude representation. We show that the ensuing standard eigenvalue problem, solved numerically, can provide an arbitrarily accurate solution for all possible motion.

Exemplary applications of Floquet theory to the related problem of stability analysis are given by Calico and Wiesel[15] (attitude dynamics), Mingori[16] (dual-spin spacecraft), and Noah and Hopkins[17] (dynamic systems).

Received 22 June 1998; revision received 1 March 1999; accepted for publication 4 April 1999. Published by the American Institute of Aeronautics and Astronautics, Inc., with permission.

*Doctoral Candidate, School of Aeronautics and Astronautics. Formerly R. Anne Beck. Student Member AIAA.

†Professor and Associate Head, School of Aeronautics and Astronautics. Member AIAA.

‡Professor, School of Aeronautics and Astronautics. Associate Fellow AIAA.

Analytic Solutions

Euler's Equations of Motion

The motion of a rigid body is governed by Euler's equations,

$$\dot{\omega}_x = \frac{M_x}{I_x} - \left(\frac{I_z - I_y}{I_x}\right)\omega_y\omega_z \tag{1}$$

$$\dot{\omega}_y = \frac{M_y}{I_y} - \left(\frac{I_x - I_z}{I_y}\right)\omega_z\omega_x \tag{2}$$

$$\dot{\omega}_z = \frac{M_z}{I_z} - \left(\frac{I_y - I_x}{I_z}\right)\omega_x\omega_y \tag{3}$$

where M_x, M_y, and M_z are torque components, ω_x, ω_y, and ω_z are angular velocity components, and I_x, I_y, and I_z are principal moments of inertia. We assume that the applied torques are constant and purely transverse ($M_z = 0$). Such transverse torques often appear in spacecraft thrusting maneuvers due to center-of-mass offset and thruster misalignment. In addition, we assume that the mass distribution is fixed, i.e., the case of the self-excited rigid body,[1] and that the body is nearly axisymmetric [$(I_x - I_y)/I_z \ll 1$]. Thus, the angular velocity about the z axis will be nearly constant

$$\omega_z \approx \omega_z(0) \tag{4}$$

For the axisymmetric case ($I_x = I_y$), Eq. (4) is exact.

With this simplification, as discussed by Randall et al.,[9] Eqs. (1) and (2) reduce to a pair of linear, constant-coefficient, ordinary differential equations with constant forcing terms. The solution for (ω_x, ω_y) is a simple sine wave, which we can write in the compact form,

$$\frac{\omega}{\omega_z} = 2\sum_{n=-1}^{1} \omega_n E_n \tag{5}$$

where

$$\omega(t) = \omega_x(t) + i\omega_y(t) \tag{6}$$

$$E_n = e^{in\kappa\tau} \tag{7}$$

$$\tau = \omega_z t \tag{8}$$

The constant κ, determined by the mass distribution, is the transverse mode frequency in units of ω_z. It ranges between $\kappa = 0$ (a sphere) and $\kappa = 1$ (a flat disk). The three nondimensional constants ω_n are

determined by the applied torques and the initial conditions through the relations

$$\kappa_x = \sqrt{\frac{I_z - I_y}{I_x}}, \qquad \kappa_y = \sqrt{\frac{I_z - I_x}{I_y}} \tag{9}$$

$$\kappa = \kappa_x \kappa_y \tag{10}$$

$$\kappa_1 = \frac{1/\kappa_x + 1/\kappa_y}{2} \tag{11}$$

$$\kappa_2 = \frac{1/\kappa_y - 1/\kappa_x}{2} \tag{12}$$

$$F = \frac{iM_x/(I_x\kappa_x) - M_y/(I_y\kappa_y)}{\omega_z^2} \tag{13}$$

$$\Omega_0 = \left(\frac{\omega_x\kappa_y + i\omega_y\kappa_x}{\omega_z}\right)\bigg|_{t=0} \tag{14}$$

$$\omega_{-1} = \frac{\kappa_2(\bar{\Omega}_0 - \bar{F})}{2} \tag{15}$$

$$\omega_0 = \frac{\kappa_1 F + \kappa_2 \bar{F}}{2} \tag{16}$$

$$\omega_1 = \frac{\kappa_1(\Omega_0 - F)}{2} \tag{17}$$

where the overbar denotes complex conjugation. Note that this solution, in which ω_x and ω_y are sinusoidal, relies on the effective constancy of ω_z. The main point of this paper is to present a solution of the kinematic problem when this is true.

Kinematic Equations

A classical method of expressing the attitude motion of a rigid body is to use a type 1: 3–2–1 Euler angle sequence.[18] The corresponding kinematic equations are

$$\dot{\phi}_x = \omega_x + (\omega_y \sin\phi_x + \omega_z \cos\phi_x)\tan\phi_y \tag{18}$$

$$\dot{\phi}_y = \omega_y \cos\phi_x - \omega_z \sin\phi_x \tag{19}$$

$$\dot{\phi}_z = (\omega_y \sin\phi_x + \omega_z \cos\phi_x)\sec\phi_y \tag{20}$$

where ϕ_x, ϕ_y, and ϕ_z are the Eulerian angles. These equations are highly nonlinear and seemingly intractable for analytical solution, although much progress has been made using linearization, e.g., by assuming ϕ_x and ϕ_y are small.[6,9]

An alternative and, for our purposes, preferable representation of the kinematics is the Cayley–Klein parameters[10,14] $[\alpha, \beta]$, which are defined in terms of the Euler angles by

$$\alpha = e^{i\phi_z/2}[\cos(\phi_x/2)\cos(\phi_y/2) - i\sin(\phi_x/2)\sin(\phi_y/2)] \tag{21}$$

$$\beta = e^{i\phi_z/2}[\cos(\phi_x/2)\sin(\phi_y/2) - i\sin(\phi_x/2)\cos(\phi_y/2)] \tag{22}$$

These two complex numbers obey the normalization $|\alpha|^2 + |\beta|^2 = 1$ as is easily confirmed from their definition.

The inverse relation, giving Euler angles in terms of Cayley–Klein parameters, is

$$\phi_x = \tan^{-1}\left[\frac{2\,\mathrm{Im}(\alpha\bar{\beta})}{|\alpha|^2 - |\beta|^2}\right] \tag{23}$$

$$\phi_y = \sin^{-1}[2\,\mathrm{Re}(\alpha\bar{\beta})] \tag{24}$$

$$\phi_z = \tan^{-1}\left[\frac{\mathrm{Im}(\alpha^2 - \beta^2)}{\mathrm{Re}(\alpha^2 - \beta^2)}\right] \tag{25}$$

The advantage of the Cayley–Klein representation is that $[\alpha, \beta]$ obey linear differential equations, in sharp contrast to Eqs. (18–20),

$$\dot{\alpha} = (i\omega_z/2)\alpha - (i\bar{\omega}/2)\beta \tag{26}$$

$$\dot{\beta} = -(i\omega/2)\alpha - (i\omega_z/2)\beta \tag{27}$$

This allows us to use the principle of linear superposition to construct general solutions for arbitrary initial conditions. Moreover, with the approximation $\omega_z = \omega_z(0)$, the coefficient $\omega(t)$ in Eqs. (26) and (27) is periodic, so that the fundamental solutions can be developed using Floquet theory, even for very large angular displacements.

Floquet Formulation and Solution of Kinematic Equations

We seek the general solution of Eqs. (26) and (27) for the Cayley–Klein parameters. These equations form a second-order, linear homogeneous system, so that there are two independent solutions. Also, by inspection, they have the symmetry that if $[\alpha, \beta]$ is a solution, then so is $[\bar{\beta}, -\bar{\alpha}]$. Hence, the general solution must have the form

$$\alpha = C_1\alpha_1 + C_2\bar{\beta}_1 \tag{28}$$

$$\beta = C_1\beta_1 - C_2\bar{\alpha}_1 \tag{29}$$

where $[\alpha_1, \beta_1]$ is any solution pair.

Finally, as seen in Eq. (5), the coefficients are periodic in τ with period $T = 2\pi/\kappa$, so that Floquet theory[12,13] applies. The essence of Floquet theory is that there will be solutions of the form

$$\alpha = e^{-is\tau}u(\tau) \tag{30}$$

$$\beta = e^{-is\tau}v(\tau) \tag{31}$$

where u and v will be periodic with period T provided that s is suitably chosen.

It follows that the general solution of Eqs. (26) and (27) can be written as

$$\alpha = C_1 e^{-is\tau}u + C_2 e^{is\tau}\bar{v} \tag{32}$$

$$\beta = C_1 e^{-is\tau}v - C_2 e^{is\tau}\bar{u} \tag{33}$$

where C_1 and C_2 are determined by the initial conditions. The $[u, v]$ are any pair of solutions of the following differential equations:

$$\frac{du}{d\tau} - i\left(s + \frac{1}{2}\right)u = -\frac{i\bar{\omega}}{2\omega_z}v \tag{34}$$

$$\frac{dv}{d\tau} - i\left(s - \frac{1}{2}\right)v = -\frac{i\omega}{2\omega_z}u \tag{35}$$

which are obtained by substituting Eqs. (30) and (31) into Eqs. (26) and (27). These equations have the symmetry that if $[u, v, s]$ is a solution then so is $[\bar{v}, -\bar{u}, -s]$.

Because $[u, v]$ are periodic, they can be represented by Fourier series,

$$u = \sum_{n=-\infty}^{\infty} u_n E_n, \qquad v = \sum_{n=-\infty}^{\infty} v_n E_n \tag{36}$$

Substituting these expansions into Eqs. (34) and (35), we get a set of recurrence relations that determine the Fourier coefficients $[u_n, v_n]$ and the eigenvalue s,

$$su_n = \left(n\kappa - \tfrac{1}{2}\right)u_n + (\bar{\omega}_{-1}v_{n-1} + \bar{\omega}_0 v_n + \bar{\omega}_1 v_{n+1}) \tag{37}$$

$$sv_n = \left(n\kappa + \tfrac{1}{2}\right)v_n + (\omega_{-1}u_{n+1} + \omega_0 u_n + \omega_1 u_{n-1}) \tag{38}$$

These relations can be arranged in the form

$$s\boldsymbol{U} = A\boldsymbol{U} \tag{39}$$

where $\boldsymbol{U} = [\ldots, u_{-1}, v_{-1}, u_0, v_0, u_1, v_1, \ldots]^T$ and A is an infinite-dimensional, pentadiagonal matrix,

$$A = \mathrm{diag}(D_{-3}, D_{-1}, D_0, D_1, D_3) \tag{40}$$

where D_0 is the main diagonal, D_1 the first superdiagonal, D_{-1} the first subdiagonal, etc. The elements of these diagonals are

$$D_0 = \left[\cdots \left(n\kappa - \tfrac{1}{2}, n\kappa + \tfrac{1}{2}\right) \cdots \right] \tag{41}$$

$$D_{-1} = \bar{D}_1 = [\cdots (\omega_0, \bar{\omega}_{-1}) \cdots] \tag{42}$$

$$D_{-3} = \bar{D}_3 = [\cdots (\omega_1, 0) \cdots] \tag{43}$$

It is easily seen that A is Hermitian, so that the eigenvalues s must be real. Moreover, we can show [most easily from Eqs. (37) and (38)] that if s_0 is an eigenvalue, then so is $\pm s_0 + N\kappa$ where N is any integer. Therefore, although there are an infinite number of eigenvalues of this infinite-dimensional matrix A, there is, in fact only one that is physically distinct. (The other eigenvalues and eigenvectors arise from a trivial renumbering of the Fourier modes.)

In practice, only a finite number of terms, $n = [-M, M]$, can be retained in the series, Eq. (36). When this is done, the $\boldsymbol{U}$ vector will be of length $4M + 2$, and the matrix A will be square of the same size. For example, the smallest such truncation, $M = 1$, yields the 6×6 matrix

$$A = \begin{bmatrix} -\kappa - \frac{1}{2} & \bar{\omega}_0 & 0 & \bar{\omega}_1 & 0 & 0 \\ \omega_0 & -\kappa + \frac{1}{2} & \omega_{-1} & 0 & 0 & 0 \\ 0 & \bar{\omega}_{-1} & -\frac{1}{2} & \bar{\omega}_0 & 0 & \bar{\omega}_1 \\ \omega_1 & 0 & \omega_0 & +\frac{1}{2} & \omega_{-1} & 0 \\ 0 & 0 & 0 & \bar{\omega}_{-1} & \kappa - \frac{1}{2} & \bar{\omega}_0 \\ 0 & 0 & \omega_1 & 0 & \omega_0 & \kappa + \frac{1}{2} \end{bmatrix}$$

corresponding to the truncated state vector

$$\boldsymbol{U} = [u_{-1} \quad v_{-1} \quad u_0 \quad v_0 \quad u_1 \quad v_1]^T$$

The truncated matrix will have $2M + 1$ equal and opposite pairs of real eigenvalues, but because the truncation breaks the translational symmetry, the eigenvalues will not be precisely related by $\pm s_0 + N\kappa$. For any given M, some of the $4M + 2$ eigenvalues will be more accurate than others.

The key questions are: how big must M be to achieve a given accuracy and how can the most accurate eigenvalue be selected? These questions will be answered in more detail in a later section, after we have looked at some numerical results. However, we can now give a rough estimate of the how big M needs to be.

For very large n, the Fourier coefficients must decrease (or the series would diverge). Thus for sufficiently large n, the dominant terms in Eq. (37) must be u_n and v_{n-1} and in Eq. (38) must be v_n and u_{n-1}. Eliminating u, we find that the ratio of alternating v coefficients must behave as

$$\frac{v_n}{v_{n-2}} \approx \frac{\omega_1 \bar{\omega}_{-1}}{(n\kappa)^2} \quad \text{as} \quad n \to \infty \tag{44}$$

with similar expressions for u and for $n \to -\infty$. This demonstrates the following two important properties.

1) The Fourier coefficients decay superexponentially for large n.

2) We must have $n > \nu/\kappa$ before the coefficients begin to decay, where $\nu = (\sum |\omega_n|^2)^{1/2}$ (or similar norm of the Fourier coefficients ω_n).

The first property says the series will converge rapidly, so that not many terms will be needed. The second property gives us a lower bound on a reasonable truncation level,

$$M \geq 1 + \nu/\kappa \tag{45}$$

Evidently, when $\nu \ll 1$, only a very few terms will be needed. A formal discussion of convergence properties of a similar problem is given by Noah and Hopkins.[17]

Small Torque Approximation

When the applied torque is small enough so that $\nu \ll 1$, the matrix A is essentially diagonal, and we can derive a simple approximate solution of Eq. (39). The result is that the Fourier coefficients form an asymptotic sequence in powers of ν. The coefficients for $|n| > 1$ are $\mathcal{O}(\nu^3)$ or smaller, so that to get $\mathcal{O}(\nu^2)$ accuracy we only need to compute the terms for $n = [-1, 0, 1]$. This can be done recursively starting with the scaling assumption $v_0 = 1$, with the result

$$n = [-1, 0, 1] \tag{46}$$

$$u_n \approx [-\bar{\omega}_1/(1+\kappa), \bar{\omega}_0, -\bar{\omega}_{-1}/(1-\kappa)] \tag{47}$$

$$v_n \approx \left[\frac{1}{\kappa} \left(\frac{\omega_0 \bar{\omega}_1}{1+\kappa} + \bar{\omega}_0 \omega_{-1} \right), 1, -\frac{1}{\kappa} \left(\bar{\omega}_0 \omega_1 + \frac{\omega_0 \bar{\omega}_{-1}}{1-\kappa} \right) \right] \tag{48}$$

At this level of approximation, $[u, v]$ are simple harmonic. The eigenvalue s, to the same order, is given by

$$s \approx \frac{1}{2} \left[1 + 4 \sum_{n=-1}^{1} \frac{|\omega_n|^2}{1 + n\kappa} \right]^{\frac{1}{2}} \tag{49}$$

It is evident from the singularities in Eqs. (47) and (48) that this solution fails when $\kappa = 0$ (sphere) and $\kappa = 1$ (plate), regardless of how small ν is. When κ is close to either extreme, the ordering of the coefficients changes, so that the $n = 2$ terms may be as large as the $n = 1$ terms.

The approximate solution given here is asymptotically equivalent to an $M = 1$ truncation of Eq. (39), but is algebraically simpler.

Numerical Results

Test Case

To test the Floquet solution, we consider a Galileo-like spacecraft maneuver. We assume the following axisymmetric mass properties[9]:

$$I_x = I_y = 3012 \text{ kg m}^2, \qquad I_z = 4627 \text{ kg m}^2 \tag{50}$$

and initial conditions

$$\omega_x(0) = \omega_y(0) = 0 \text{ rad/s}, \qquad \omega_z(0) = 0.33 \text{ rad/s} \tag{51}$$

$$\phi_x(0) = \phi_y(0) = \phi_z(0) = 0 \text{ rad} \tag{52}$$

Transverse torque can arise from a center-of-mass offset of the main engine. We select a very large transverse torque (about 150 times that of the Galileo) to demonstrate the theory for an extreme case where the Euler angles (ϕ_x, ϕ_y) approach 90 deg

$$M_x = 225 \text{ Nm}, \qquad M_y = 0, \qquad M_z = 0 \tag{53}$$

For this test case we note that the inertia parameter $\kappa = 0.5362$ and Eqs. (15–17) yield the following constant values:

$$\omega_{-1} = 0, \qquad \omega_0 = 0.6397i, \qquad \omega_1 = -0.6397i \tag{54}$$

Baseline Numerical Integration

Because we expect the Floquet solution to be highly accurate, we need a very precise method to test it. We employ an adaptive Runge–Kutta fourth/fifth-order integration method using double precision accuracy for the following simulations. In each case the accuracy is controlled by a relative tolerance of 1×10^{-12} and an absolute tolerance of 1×10^{-14}. For our baseline numerical integration we integrate Eqs. (1–3) and (18–20). The errors in the baseline numerical integration are on the order of 10^{-12} rad for the Euler angles.

Discussion of Test Case

This discussion pertains to the test case Eqs. (50–52) with

$$M = 7 \tag{55}$$

From Floquet theory we know that the parameters u and v are periodic with period $T = 2\pi/\kappa$. In Fig. 1 we plot the real (solid line) and the imaginary (dashed line) parts of the solution for Eqs. (34) and (35) for one period.

The Cayley–Klein parameters α and β, obtained using Eqs. (32) and (33), are not periodic in general. The real and the imaginary parts of α and β are plotted in Fig. 2 for two periods of the u, v solution ($2T/\omega_z$). We note that the plots satisfy the normalization constraint that $|\alpha|^2 + |\beta|^2 = 1$.

Figure 3a shows two solutions for the Euler angle ϕ_x: the Floquet solution [obtained using the solutions for α and β and Eq. (23)] and the baseline numerical integration. Because the results are indistinguishable at this scale, we show the difference between the results in Fig. 3b. The maximum error is about 5.5×10^{-5} rad out of 1.6 rad (at $t = 16$ s) or about 0.003%.

A similar comparison for the spin angle ϕ_z is shown in Fig. 4. We note that ϕ_z is very large for large values of time. For convenience we introduce a smaller angle Φ_z, obtained by subtracting off the linearized solution for ϕ_z

$$\Phi_z \equiv \phi_z - \omega_z t \tag{56}$$

In Fig. 4a, we show the baseline solution for the angle Φ_z and the Floquet solution obtained using α and β and Eqs. (25) and (56). To check the accuracy, we again show the difference between the two solutions in Fig. 4b. Here we see the error is about 3×10^{-6} rad out of 1 rad (at $t = 9$ s) or 0.0003%. Because the errors in the baseline solution are $\mathcal{O}(10^{-12})$ rad, the difference represents the true error in the Floquet solution.

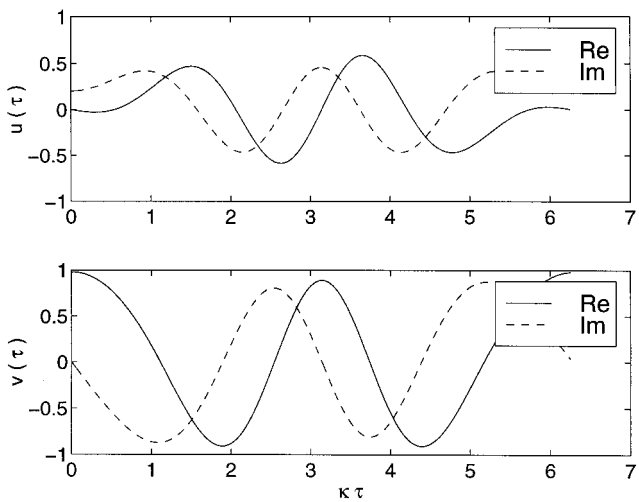

Fig. 1 One period of u and v for test case.

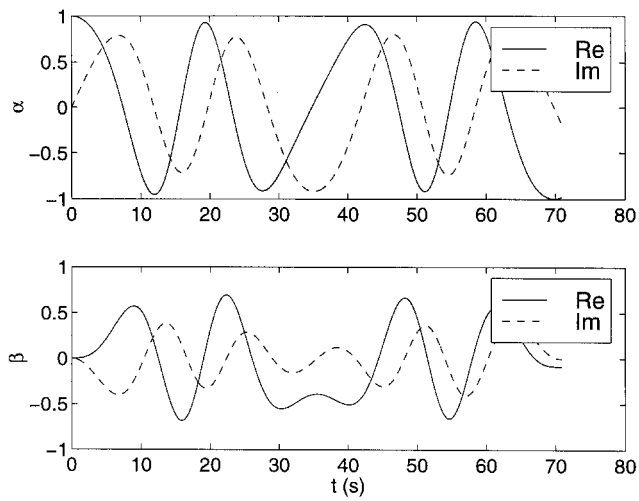

Fig. 2 Cayley–Klein functions α and β for test case.

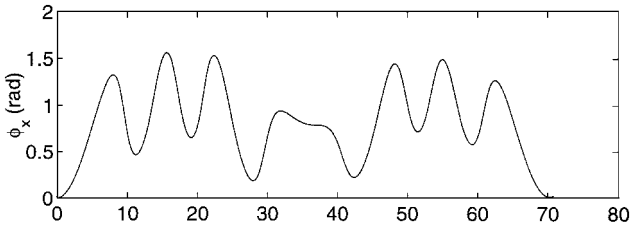

a) Baseline and Floquet solutions

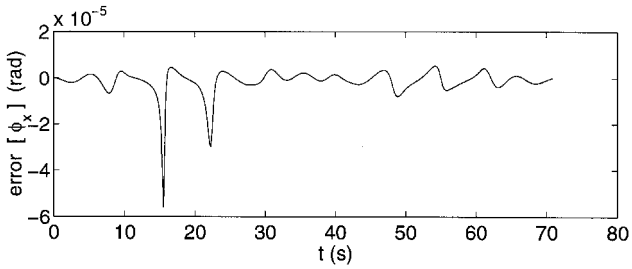

b) Baseline minus Floquet solution

Fig. 3 Euler angle ϕ_x for test case.

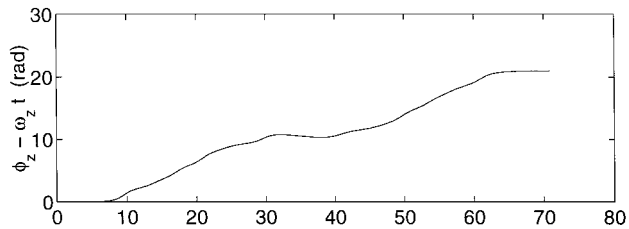

a) Baseline and Floquet solutions

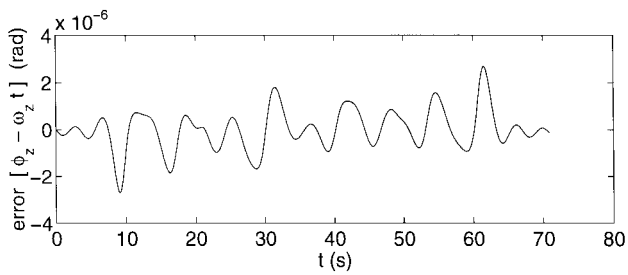

b) Baseline minus Floquet solution

Fig. 4 Angle $\Phi_z = \phi_z - \omega_z t$ for test case.

Accuracy Assessment

To study the effects of M on the accuracy of the Floquet solution, we conduct the following parametric study. We first fix a value for M. We then compute the baseline numerical integration and Floquet solutions for ϕ_x using transverse torque M_x in the range of 0–225 Nm. For each of these trajectories, we compute the difference between the two solutions. In Fig. 5, we plot percent error vs the maximum absolute value $|\phi_x|_{\max}$. As expected, the error increases as the angle increases; larger values of M result in smaller errors. We note that the plateau at the bottom of Fig. 5 occurs due to the errors in the baseline numerical integration and not the Floquet solution. (For large values of M, the Floquet solution is more accurate than the baseline solution.) Also as ϕ_x approaches 90 deg, the error increases rapidly due to the well-known Euler angle singularity.

A similar study is conducted for the angle Φ_z. In Fig. 6, percent error vs the maximum absolute value $|\Phi_z|_{\max}$ is plotted. Again, the error increases as the angle increases, and larger values of M result in smaller errors. A similar numerical integration plateau occurs.

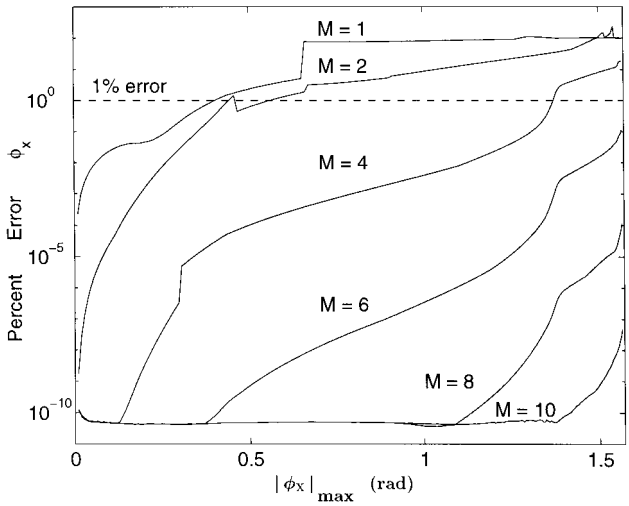

Fig. 5 Percent error in maximum absolute value of ϕ_x for various transverse torques (axisymmetric case).

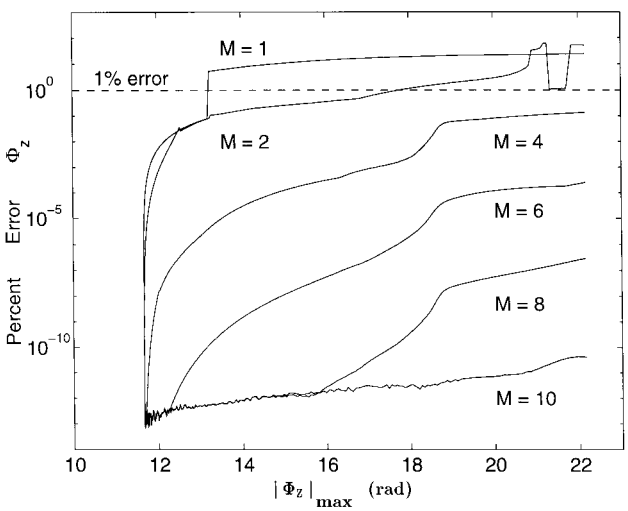

Fig. 6 Percent error in maximum absolute value of Φ_z for various transverse torques (axisymmetric case).

Figures 5 and 6 can be used to choose M to achieve a given accuracy in the Floquet solution, but only for the test case. For the general case it would be useful to have a method that selects M for a desired accuracy.

Eigenvector Selection

At any given truncation level M, there are $2M+1$ distinct values of s^2 that arise from solving Eq. (39). Some of these values will be better than others, and so we must sort the wheat from the chaff. The essential idea is that because we centered the truncation about $n=0$, then those eigenvectors that are most nearly centered about $n=0$ should be most accurate. We illustrate this in Figs. 7 and 8, which show 2 of the 30 eigenvector spectra for an $M=7$ truncation of the test case. In Fig. 7, the peak occurs near the left edge of the window, and so the neglected terms in $n<-7$ are not small, and the solution is poor. In Fig. 8, the peak is near the middle of the window, and the neglected terms on both the left and right ($|n|>7$) are clearly less than 10^{-5} in magnitude. This is the best we can do with $M=7$.

The described selection process can be automated by measuring the error in a spectrum, ϵ, from the size of its end elements,

$$\epsilon = |u_{-M}| + |v_{-M}| + |u_M| + |v_M| \tag{57}$$

There will be $4M+2$ values of ϵ; the best solution is the one for which ϵ is minimum. For the test case with $M=7$, this optimal solution is shown in Fig. 8. Note that the poor result in Fig. 7 corresponds to $s+6\kappa=0.1183$, which is 5% off the target of $s=0.1245$.

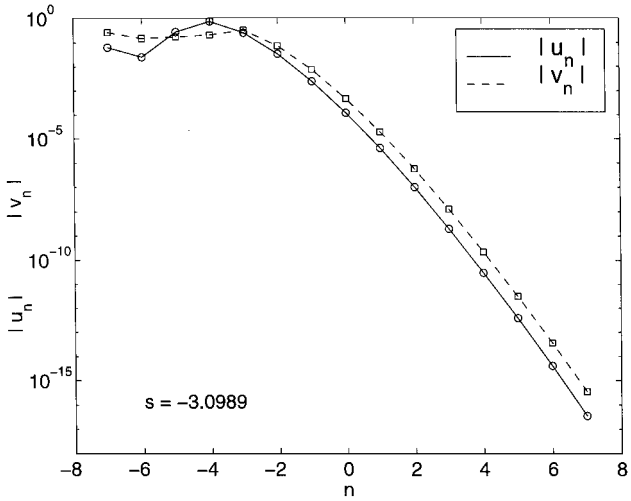

Fig. 7 Suboptimal eigenvalue/eigenvector selection of M_x = 225 Nm, M = 7.

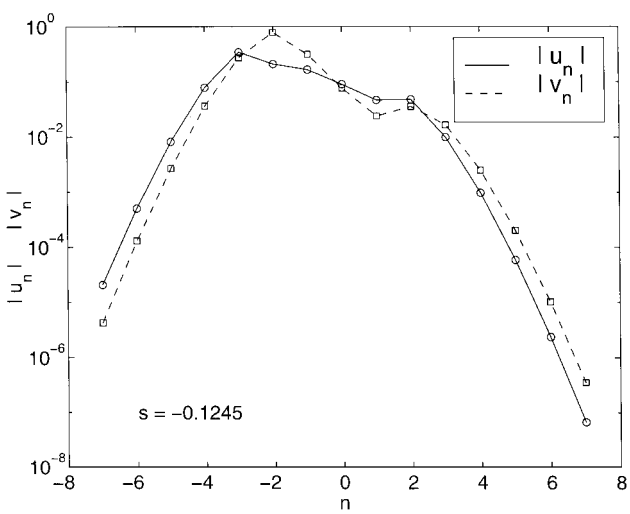

Fig. 8 Optimal eigenvalue/eigenvector selection of M_x = 225 Nm, M = 7.

The occurrence of errors of this order is to be expected from the size of the $n=-7$ Fourier coefficients (about 10^{-1}) seen at the left in Fig. 7.

Automatic Error Control

Having shown how to select the best eigensolution at a given truncation, we can easily see how to automatically select M to give any specified accuracy in the solution.

1) Pick a tolerance ϵ_{max} and the smallest reasonable truncation: $M=1+\nu/\kappa$.

2) Solve the truncated eigenproblem, selecting that vector with minimum error, ϵ_{min}.

3) If $\epsilon_{min}<\epsilon_{max}$, stop. If $\epsilon_{min}>\epsilon_{max}$, increase M; repeat steps 2 and 3.

The assumption made in this algorithm is that the errors in the solution (for u and v) are smaller than the last retained Fourier coefficients.

It is, naturally, wasteful to compute all $4M+2$ eigensolutions when all but one are thrown away. For this reason, a practical approach is to use an iterative eigensolver that computes only a few of the eigenvalues closest to the previous optimum. On the first step, the center eigenvalue is set at $s=\frac{1}{2}$, based on the small-torque solution, Eq. (49).

Results for a Nearly Axisymmetric Case

It is only natural to be curious as to what happens when the aforementioned Floquet solution is applied to a more realistic case. We

choose the following nearly axisymmetric mass properties (which are closer to the values of the Galileo spacecraft[9]):

$$I_x = 3012\,\text{kg m}^2, \qquad I_y = 2761\,\text{kg m}^2, \qquad I_z = 4627\,\text{kg m}^2 \tag{58}$$

with a moderately large transverse torque

$$M_x = 100\,\text{Nm}, \qquad M_y = 0, \qquad M_z = 0 \tag{59}$$

and use the same initial conditions as the earlier test case. Here we note that the inertia parameter κ is slightly larger with a value of

$$\kappa = 0.6020 \tag{60}$$

and Eqs. (15–17) yield the following smaller ω_n values:

$$\omega_{-1} = 0.0036i, \qquad \omega_0 = 0.2461i, \qquad \omega_1 = -0.2496i \tag{61}$$

We see in Fig. 9 that ω_z is periodic with a small-amplitude fluctuation of 5%, not constant as assumed from Eq. (4). Figures 10 and 11 show the results for ϕ_x and Φ_z, respectively. We notice that the Floquet solution seems to track reasonably well for a while then diverges from the baseline solution. However, the accuracy is significantly poorer (than the axisymmetric test case), even in the first oscillation. We know that this error is not due to truncation because varying M from 2 to 10 makes no difference. The reason for the inaccuracy is because ω_z is not constant. It is possible to improve the solution by including perturbations to ω_z due to the neglected term in Eq. (3). The additional terms will be periodic, and so Floquet theory still applies; however, the analysis is beyond the scope of the current paper.

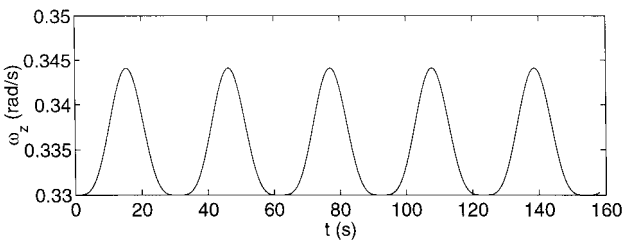

Fig. 9 Angular velocity ω_z for nearly axisymmetric case.

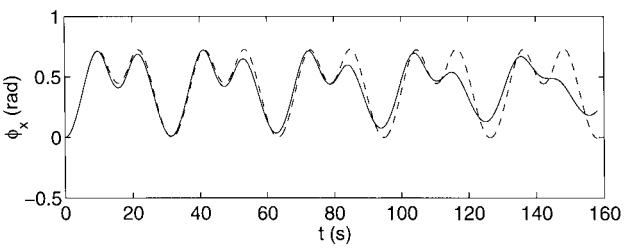

Fig. 10 Euler angle ϕ_x for nearly axisymmetric case.

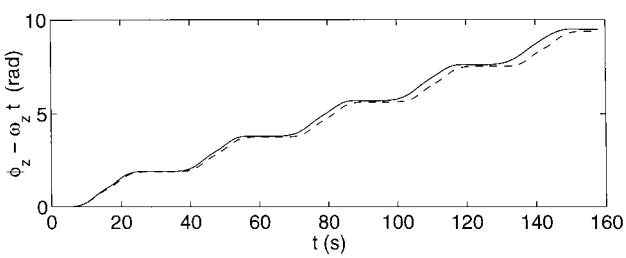

Fig. 11 Angle $\Phi_z = \phi_z - \omega_z t$ for nearly axisymmetric case.

The amplitude of the ω_z oscillations is proportional to the square of the applied torque. Therefore, if we reduce M_x from 100 to 10 Nm, the 5% fluctuation seen in Fig. 9 drops to 0.05%. Based on simulations over the same duration as Fig. 10, the errors in the Euler angles drop significantly [to $\mathcal{O}(10^{-3})$ rad]. Therefore, even though large errors are possible in the nearly axisymmetric case when large torques are applied, the present method is still quite accurate and useful for typical spacecraft maneuvers with small transverse torques.

Conclusions

The Floquet solution presented, based on a Cayley–Klein formulation of the kinematic equations, is much more accurate and efficient than any previously found linear solutions, even when the angular excursion of the spin axis is large. The major assumption is that the spin rate is constant. This method is highly accurate for the axisymmetric case regardless of how large the torque is; however, when the theory is applied to the nearly axisymmetric case, the errors are small only when the torques are small. This solution may find applications in onboard computations of spacecraft maneuvers and in maneuver analysis and optimization.

Acknowledgments

This research is supported in part by NASA Headquarters under Grant NGT5-50110 (NASA program official Dolores Holland).

References

[1]Leimanis, E., *The General Problem of the Motion of Coupled Rigid Bodies About a Fixed Point*, Springer–Verlag, New York, 1965, Chap. 2.

[2]Larson, V., and Likins, P. W., "Closed-Form Solutions for the State Equation for Dual-Spin and Spinning Spacecraft," *Journal of the Astronautical Sciences*, Vol. 21, No. 5–6, 1974, pp. 244–251.

[3]Kraige, L. G., and Junkins, J. L., "Perturbation Formulations for Satellite Attitude Dynamics," *Celestial Mechanics*, Vol. 13, No. 1, 1976, pp. 39–64.

[4]Kraige, L. G., and Skaar, S. B., "A Variation of Parameters Approach to the Arbitrarily Torqued, Asymmetric Rigid Body Problem," *Journal of the Astronautical Sciences*, Vol. 25, No. 3, 1977, pp. 207–226.

[5]Kane, T. R., and Levinson, D. A., "Approximate Solution of Differential Equations Governing the Orientation of a Rigid Body in a Reference Frame," *Journal of Applied Mechanics*, Vol. 54, No. 1, 1987, pp. 232–234.

[6]Longuski, J. M., "Real Solutions for the Attitude Motion of a Self-Excited Rigid Body," *Acta Astronautica*, Vol. 25, No. 3, 1991, pp. 131–140.

[7]Or, A. C., "Injection Errors of a Rapidly Spinning Spacecraft with Asymmetries and Imbalances," *Journal of the Astronautical Sciences*, Vol. 40, No. 3, 1992, pp. 419–427.

[8]Longuski, J. M., and Tsiotras, P., "Analytic Solution of the Large Angle Problem in Rigid Body Attitude Dynamics," *Journal of the Astronautical Sciences*, Vol. 43, No. 1, 1995, pp. 25–46.

[9]Randall, L. A., Longuski, J. M., and Beck, R. A., "Complex Analytic Solutions for a Spinning Rigid Body Subject to Constant Transverse Torques," *Proceedings of the AAS/AIAA Astrodynamics Specialist Conference*, Advances in the Astronautical Sciences Paper 95-373, Univelt, Inc., San Diego, CA, Aug. 1995.

[10]Shuster, M. D., "A Survey of Attitude Representations," *Journal of the Astronautical Sciences*, Vol. 41, No. 4, 1993, pp. 439–518.

[11]Tsiotras, P., and Longuski, J. M., "A New Parameterization of the Attitude Kinematics," *Journal of the Astronautical Sciences*, Vol. 43, No. 3, 1995, pp. 243–262.

[12]Meirovitch, L., *Methods of Analytical Dynamics*, McGraw–Hill, New York, 1970, pp. 264–280.

[13]Nayfeh, A. H., and Balachandran, B., *Applied Nonlinear Dynamics*, Wiley, New York, 1995, pp. 158–172.

[14]Goldstein, H., *Classical Mechanics*, Addison–Wesley, Reading, MA, 1980, pp. 148–158.

[15]Calico, R. A., and Wiesel, W. E., "Time Periodic Attitude Control Problems," *Journal of Guidance, Control, and Dynamics*, Vol. 7, No. 6, 1984, pp. 671–676.

[16]Mingori, D. L., "Effects of Energy Dissipation on the Attitude Stability of Dual-Spin Satellites," *AIAA Journal*, Vol. 7, No. 1, 1969, pp. 20–27.

[17]Noah, S. T., and Hopkins, G. R., "A Generalized Hill's Method for Stability Analysis of Parametrically Excited Dynamic Systems," *Journal of Applied Mechanics*, Vol. 49, No. 1, 1982, pp. 217–223.

[18]Wertz, J. R., *Spacecraft Attitude Determination and Control*, D. Reidel, Dordrecht, The Netherlands, 1980, pp. 760–766.